



Interacting bosons in one dimension and the applicability of Luttinger-liquid theory as revealed by path-integral quantum Monte Carlo calculations

Adrian Del Maestro and Ian Affleck

Department of Physics and Astronomy, University of British Columbia, Vancouver, British Columbia, Canada V6T 1Z1

(Received 23 July 2010; revised manuscript received 15 August 2010; published 26 August 2010)

Harmonically trapped ultracold atoms and ^4He in nanopores provide different experimental realizations of bosons in one dimension, motivating the search for a more complete theoretical understanding of their low-energy properties. Worm algorithm path-integral quantum Monte Carlo results for interacting bosons restricted to the one dimensional continuum are compared to the finite temperature and system size predictions of Luttinger-liquid theory. For large system sizes at low temperature, excellent agreement is obtained after including the leading irrelevant interactions in the Hamiltonian which are determined explicitly.

DOI: [10.1103/PhysRevB.82.060515](https://doi.org/10.1103/PhysRevB.82.060515)

PACS number(s): 67.10.Fj, 67.25.bh, 05.30.Jp, 02.70.Ss

Luttinger-liquid (LL) theory¹ provides a universal description of interacting fermions or bosons at sufficiently low energies in one dimension (1D). Recently, exciting possibilities for experimental realizations of Luttinger liquids have appeared, involving ultracold atoms in cigar-shaped traps,² screw dislocations in solid ^4He (Ref. 3), and helium-4 confined to flow in nanopores.⁴ While the latter experiment examines a system that is highly out of equilibrium, future iterations⁵ could be well described by a translationally invariant model of interacting bosons. There have been numerous numerical studies of 1D fermion models on lattices using exact diagonalization, Monte Carlo, and density matrix renormalization-group methods, but numerical results on free space interacting bosons at nonzero temperature, T , are much rarer. Exact studies in the continuum may provide insights, specifically on issues of dimensional crossover in nanopores.⁶ Zero-temperature variational Monte Carlo calculations for the 1D case were reported in Ref. 7 and finite T worm algorithm path-integral Monte Carlo (WA-PIMC) simulations for a screw dislocation³ have claimed the observation of LL behavior. In order to systematically explore the regime of energies and pore lengths, where LL behavior may occur we have performed WA-PIMC simulations on the N -particle Hamiltonian

$$H = -\frac{1}{2m} \sum_{i=1}^N \nabla_i^2 + \frac{1}{2} \sum_{i,j=1}^N V(|\vec{r}_i - \vec{r}_j|) \quad (1)$$

in 1D with periodic boundary conditions on an interval of length L in angstroms and we will work in units where $\hbar = k_B = 1$. The WA-PIMC method, recently introduced by Boninsegni *et al.*⁸ extends the original PIMC algorithm of Ceperley⁹ to include configurations of the single-particle Matsubara Green's function, allowing for intermediate particle trajectories which are not periodic in imaginary time. The inclusion of such trajectories yield an efficient and robust grand canonical quantum Monte Carlo (QMC) technique that accurately incorporate complete quantum statistics and provides exact and unbiased estimations of many physical observables at finite temperature. In the WA-PIMC simulations performed here, the short-range repulsive interaction $V(r) = (g/\sqrt{\pi a})e^{-r^2/4a^2}$ is chosen for convenience to be Gauss-

ian with integrated strength $2g$ and spatial extent a . The numerical values of all microscopic parameters were optimized to ensure an experimentally relevant and efficient simulation at low energies, where the temperature is much smaller than both the kinetic (E_K/N) and potential (E_V/N) energy per particle. To obtain $E_K/N \sim E_V/N \sim 5$ K we have fixed the chemical potential at $\mu = 24$ K with $2g = 20$ K and the interaction width $a \approx 0.03$ Å to be much less than the resulting interparticle separation, $1/\rho_0 \approx 0.67$ Å for particles of mass $m = 0.25$ Å⁻² K⁻¹ (near that of ^4He in these units).

Luttinger-liquid theory uses a low-energy effective harmonic Hamiltonian to capture the quantum hydrodynamics of a microscopic 1D system in terms of two bosonic fields, $\theta(x)$ and $\phi(x)$ representing the density and phase oscillations of a particle field operator

$$H_{LL} - \mu N = \frac{1}{2\pi} \int_0^L dx [v_J (\partial_x \phi)^2 + v_N (\partial_x \theta)^2], \quad (2)$$

where the velocities v_J and v_N are fixed by the microscopic details of the underlying high-energy model. If the system exhibits Galilean invariance, $v_J = \pi \rho_0 / m$ and $v_N = 1 / (\pi \rho_0^2 \kappa)$, where ρ_0 and κ are the density and adiabatic compressibility in the limit $L \rightarrow \infty$, $T \rightarrow 0$.¹

In this study we find that the mean number of particles at finite temperature $\langle N \rangle$ exhibits corrections to scaling that are *not* captured by Eq. (2). Instead, through a detailed analysis of the super- and normal-fluid components of the one dimensional repulsive Bose gas, we argue that the observed deviations from scaling result from higher order “irrelevant” operators that should be included in the low-energy effective Hamiltonian.

Although the QMC performed here allows access to a large number of properties of the microscopic system, in order to study the applicability of the effective model in Eq. (2) it will be enough to focus on the probability distributions for number and phase fluctuations in the grand canonical ensemble. Within the LL theory, these are most easily derived by performing a mode expansion of $\theta(x)$ and $\phi(x)$ for periodic boundary conditions indexed by wave vector $q = 2\pi n/L$ (see Ref. 1). The grand partition function $\mathcal{Z} = \text{Tr} \exp[-(H_{LL} - \mu N)/T]$ is found to be

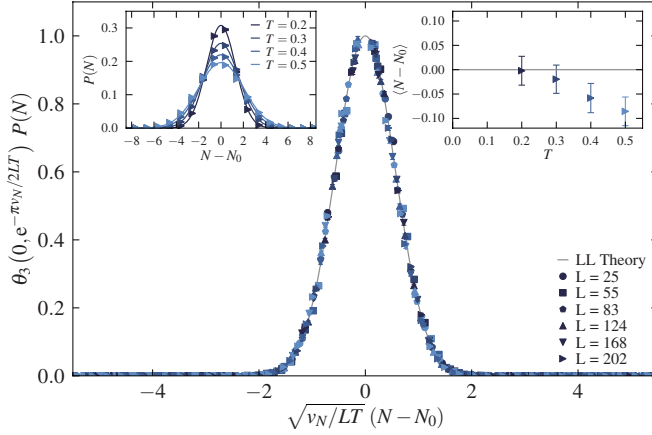


FIG. 1. (Color online) QMC data (symbols) combined with Luttinger-liquid predictions (solid lines) for the particle number probability distribution at fixed system size (upper left inset), scaling of the particle number probability distribution (main panel), and the temperature dependence of the mean number of particles (upper right inset) measured with respect to the ground-state value $N_0 = \rho_0 L$.

$$\mathcal{Z} = e^{-g_0 L/T} e^{\pi v/6LT} \sum_{N \geq 0} e^{-\pi v_N(N-N_0)^2/2LT} \times \sum_J e^{-\pi v_J J^2/2LT} \prod_{n \neq 0} (1 - e^{-2\pi v|n|/LT})^{-1}, \quad (3)$$

where $N_0 = \rho_0 L$, J is an even integer indexing topological excitations (winding) of the phase field ϕ , g_0 is the nonuniversal ground-state Gibbs free-energy per unit length, and v is the phonon velocity given by the algebraic mean of v_J and v_N : $v = \sqrt{v_J v_N}$. LL theory is unable to predict the nonuniversal μ dependence of the density in the thermodynamic limit. By tracing out winding and phonon modes, which cannot affect the density, we immediately arrive at an expression for the particle number probability distribution

$$P(N) = \frac{e^{-\pi v_N/2LT(N-N_0)^2}}{\theta_3(0, e^{-\pi v_N/2LT})}, \quad (4)$$

where $\theta_3(z, q)$ is a Jacoby Theta function of the third kind.

An immediate consequence of Eq. (4) is that LL theory predicts that the average number of particles exhibits essentially no dependence on T (Ref. 10) and it is on the validity of this prediction that we focus our attention below. An equivalent expression for $P(J)$ can be derived in the same manner. However, it will be more useful to work with a dual coordinate for J known as the winding number W , which is easily measured in the QMC (Ref. 11) through the wrapping of imaginary time particle trajectories around the physical boundaries of the sample

$$P(W) = \frac{e^{-\pi LT/2v_J W^2}}{\theta_3(0, e^{-\pi LT/2v_J})}. \quad (5)$$

The strange *inverse* Boltzmann form of this distribution can be understood by noting that in one dimension, the superfluid density is proportional to the second moment of the winding number distribution¹¹ and it is only when fluctua-

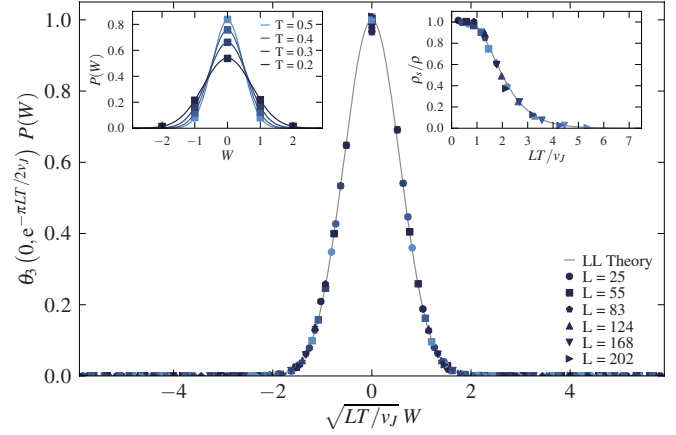


FIG. 2. (Color online) QMC data (symbols) combined with Luttinger-liquid predictions (solid lines) for the winding number probability distribution at fixed system size (upper left inset), scaling of the winding number probability distribution (main panel), and the superfluid fraction as a function of the dimensionless scaling variable LT/v_J (upper right inset).

tions of the phase field ϕ are suppressed (phase coherence with $\langle J \rangle \sim 0$) that the system will acquire a finite superfluid response. As a consequence of Eq. (5), the superfluid fraction will be a pure scaling function of v_J/LT given by¹²

$$\frac{\rho_s}{\rho} = 1 - \frac{\pi v_J}{LT} \left| \frac{\theta_3'(0, e^{-2\pi v_J/LT})}{\theta_3(0, e^{-2\pi v_J/LT})} \right|, \quad (6)$$

where $\theta_j'(z, q) \equiv \partial_z^2 \theta_j(z, q)$.

The above theoretical predictions can be verified by investigating the particle and winding number probability distributions measured in the QMC for a range of temperatures and system sizes. It is crucial to recognize that the *parameters* of LL theory $v_{J,N}$, have no temperature or finite-size dependence and depend only on the microscopic details of the high energy theory in Eq. (1). Both $P(N)$ and $P(W)$ are scaling functions of $LT/v_{J,N}$, and fits of numerical data for an individual system size at fixed temperature *must* produce values of v_J and v_N that work equally well at all L and T provided the system is in a regime where the LL theory of Eq. (2) is applicable. Figures 1 and 2 present a summary of our QMC data for $L=25-202$ Å and $T=0.2-0.5$ K. The insets in the upper left-hand corner of these figures show the result of fitting to Eqs. (4) and (5) yielding $v_J=18.88(2)$ Å K and $v_N=7.7(2)$ Å K, which combine to give a Luttinger parameter of $K=\sqrt{v_N/v_J}=0.64(4)$, where the number in brackets gives the uncertainty in the final digit. The presence of Galilean invariance relates v_J and ρ_0 and we find the zero-temperature equilibrium density to be $\rho_0=1.5028(1)$ Å⁻¹. The main panel in both plots exhibits data collapse that appears to be consistent with the scaling predictions of LL theory. However, a closer look at the average number of particles as a function of temperature for $L=202$ Å (Fig. 1 upper right inset) clearly shows that as the temperature is increased at fixed chemical potential, the mean particle number is decreasing, in stark contradiction with the prediction of Eq. (4). Conversely, scaling in the winding number sector

shows no such deviations and the computed superfluid fraction ρ_s/ρ plotted as a function of the dimensionless scaling variable LT/v_J (Fig. 2 upper right inset) is indistinguishable from the LL prediction of Eq. (6).

At sufficiently low T and large L , corrections to scaling should be described by the leading irrelevant interactions added to the Hamiltonian of Eq. (2). Recently, such corrections were shown to lead to qualitative modifications of the spectral function for fermions.¹³ Assuming that all interactions are short range, correcting terms come from an expansion of the kinetic energy in Eq. (1) and are related to band curvature effects. The lowest order correction to the LL Hamiltonian containing three derivatives, consists of two operators

$$H' = \frac{1}{2\pi^2\rho_0} \int_0^L dx [v_J(\partial_x\phi)^2\partial_x\theta + \lambda v_N(\partial_x\theta)^3], \quad (7)$$

where the coefficient of the first term is constrained by Galilean invariance. The form of H' could also have been inferred on phenomenological grounds alone, as these two terms are the only dimension three operators that are allowed by parity under which $\theta \rightarrow -\theta$, $\phi \rightarrow \phi$, and $x \rightarrow -x$. Higher fourth-order operators can also be included and are formally required for stability but are suppressed by an additional power of system size. Equation (7) is sufficient to predict the lowest order corrections to physical quantities which will manifest as scaling functions of $LT/v_{J,N}$ times an inverse factor of N_0 , which we assume is large. The dimensionless factor λ in the second coefficient can be determined¹⁴ by noting that in the ground state, if we shift the chemical po-

tential by an infinitesimal amount $\mu \rightarrow \mu + \delta\mu$ there will be a corresponding shift in the density $\rho_0 \rightarrow \rho_0 + \delta\rho_0$ governed by the thermodynamic relation $\delta\rho_0 = \rho_0^2\kappa\delta\mu$. Keeping terms to $O(\delta\mu)$ in an expansion of the ground-state Gibbs free energy for $H_{LL}+H'$ we find $\lambda = (\pi\rho_0/3)\partial_\mu v_N = (\rho_0/3)\partial_\mu(\rho_0^2\kappa)^{-1}$.

The influence of the corrections on thermodynamic quantities can be most easily understood by again performing a mode expansion of the bosonic fields θ and ϕ . Gradients of θ are related to fluctuations of the particle number away from its mean value $\partial_x\theta \sim N - N_0$ and thus the addition of linear and cubic terms will cause both a shift and skew in the particle number probability distribution $P(N)$ in Eq. (4) without changing its width. On the other hand, the only corrections at this order to the winding number distribution $P(W)$ would have to come from the first term in Eq. (7), but due to the linear power of $\partial_x\theta$, which accompanies it as a multiplicative factor, any trace over the number of particles when computing the grand partition function would cause its effects to average to zero. This is exactly the qualitative behavior we observed from the analysis of our numerical results.

In order to quantify these arguments, we may calculate the deviation in the mean number of particles $\langle N - N_0 \rangle$ in a perturbative expansion of $H_{LL}+H'$ in the inverse system size $1/L$.¹⁵ This is accomplished by correcting the number probability distribution $P(N)$ in Eq. (4) to order $1/L$ and computing the relevant average with result

$$\langle N - N_0 \rangle = -\frac{1}{N_0} \Phi_N \left(\frac{LT}{v_N}, \frac{LT}{v_J}, \lambda \right), \quad (8)$$

where

$$\begin{aligned} \Phi_N(x, y, \lambda) = & \frac{2x}{\pi} \left\{ \lambda \left[x \partial_x \ln \theta_3(0, e^{-\pi/2x}) \right]^2 + x^2 \partial_x^2 \ln \theta_3(0, e^{-\pi/2x}) + 2x \partial_x \ln \theta_3(0, e^{-\pi/2x}) \right\} \\ & - \left[\frac{1}{2} (3\lambda + 1) (y \partial_x + x \partial_y) \ln \eta(i\sqrt{xy}) - y \partial_y \ln \theta_3(0, e^{-2\pi/y}) \right] x \partial_x \ln \theta_3(0, e^{-\pi/2x}) \end{aligned} \quad (9)$$

is a universal scaling function with $\eta(ix)$ the Dedekind eta function. This expression has a simple asymptotic form in the thermodynamic limit where $LT/v_{J,N} \rightarrow \infty$

$$\Phi_N \left(\frac{LT}{v_N} \rightarrow \infty, \frac{LT}{v_J} \rightarrow \infty, \lambda \right) \rightarrow \frac{K}{12} (3\lambda + 1) \left(\frac{LT}{v_N} \right)^2 \quad (10)$$

and $K = \sqrt{v_N/v_J}$ is the LL parameter. It is now immediately clear that when Eq. (10) is combined with Eq. (8) a temperature-dependent correction to the mean density of particles will persist, even in the thermodynamic limit

$$\langle \rho - \rho_0 \rangle \rightarrow -\frac{K}{12\rho_0 v_N^2} (3\lambda + 1) T^2. \quad (11)$$

Indeed, from simple thermodynamic arguments one expects $\rho = -(1/L)\partial_\mu G$, where G , the Gibbs free energy, can be

calculated for a harmonic LL from Eq. (3) to be $G = g_0 L - (\pi L/6v) T^2$ in the limit $LT/v \rightarrow \infty$. Performing the partial derivative of G with respect to the chemical-potential recovers the asymptotic value in Eq. (11).

We may now test how well the extended Luttinger-liquid Hamiltonian $H_{LL}+H'$ captures these effects by comparing the scaling function Φ_N with our numerical data. The result is shown in Fig. 3, where we have extracted the value of $\lambda = 0.19(4)$ by refitting a perturbatively corrected number probability distribution to the QMC results using the previously extracted $v_{J,N}$. The agreement between the numerical QMC data (symbols) and the prediction of Eq. (9) (solid line) is found to have a reduced maximum-likelihood estimator of $\chi^2 \approx 0.85$. Seemingly large uncertainties in Fig. 3 are misleading as Φ_N is a correction related to the difference of two large and nearly equal numbers with indi-

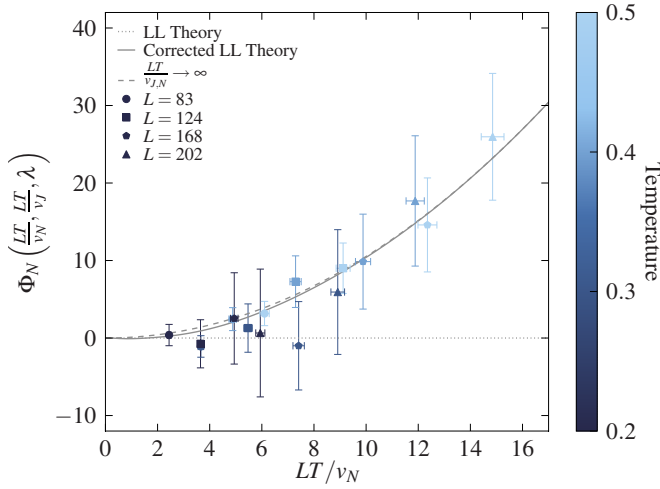


FIG. 3. (Color online) QMC data (symbols) combined with predictions from the harmonic (dotted line) and corrected anharmonic (solid line) Luttinger-liquid theory for the universal scaling function Φ_N . The dashed line shows the asymptotic result in the thermodynamic limit from Eq. (10).

vidually small stochastic errors ($<0.01\%$) resulting from over 100 K CPU hours. Poorer agreement at low temperatures is a reflection of the difficulty of performing ergodic simulations of nearly integrable systems.¹⁶ Further evidence of the statistical significance is garnered by examining the goodness of fit of the QMC data to $\Phi_N=0$ predicted by harmonic LL theory, yielding an extremely unlikely value of $\chi^2 \approx 6.2$.

A nonzero Φ_N is just one of many scaling functions that could be investigated for evidence of nonharmonic LL behavior. For example, if the QMC was confined to the canonical ensemble via importance sampling, a parallel analysis could be carried out for $\langle \mu - \mu_0 \rangle \sim (1/N_0)\Phi_\mu(LT/v_N, LT/v_i)$ via a numerical investigation of $\partial_N F$ at fixed L , where F is the Helmholtz free energy.

It is well known that an analytical solution of the delta-function interacting Bose gas can be obtained via Bethe Ansatz (BA) (Ref. 17) where the phonon velocity v can be extracted from an analysis of the linear coefficient of the long-wavelength dispersion relation.¹⁸ It seems prudent to

place our numerical data in this context and for the mass, interaction strength, and chemical potential used in the simulations, the $T \rightarrow 0, L \rightarrow \infty$ solution gives a Luttinger parameter of $K_{BA} \approx 0.6299$ and cubic operator coefficient $\lambda_{BA} \approx 0.1272$. The numbers extracted here of $K=0.64(4)$ and $\lambda=0.19(4)$ agree relatively well within error bars but their systematically larger values are related to the finite interaction width a employed in the QMC. This trend can be quantified by performing the simulation for increasingly long-range interactions (although still requiring that $a\rho_0 \ll 1$) and for $a\rho_0 \approx 0.06$ we find $K=0.75(2)$ pushing us toward a regime with enhanced charge-density wave order.

In addition to allowing for the study of finite-range interactions, Monte Carlo methods can also provide details on correlation functions that are not accessible via Bethe Ansatz.⁷ Unbiased measurements of the pair-correlation function and single-body density matrix computed in the Monte Carlo are fully consistent with the predictions of LL theory and will be reported on elsewhere.¹²

In conclusion, we have performed large-scale grand canonical worm algorithm path-integral Monte Carlo simulations of one-dimensional repulsive soft-core bosons in the continuum at fixed chemical potential. We have shown that the finite-size and temperature-scaling behavior of the superfluid density can be fully understood in terms of the low-energy effective harmonic Luttinger-liquid theory provided the temperature is sufficiently small when compared to both the kinetic and potential energy per particle and the system is large enough to overcome the effects of any finite-size gaps. However, we have argued that the temperature dependence of the mean particle density, a quantity that can be easily measured in experiments on low-dimensional bosonic systems, exhibits corrections to scaling that can only be adequately accounted for by extending the theory to include leading order irrelevant operators.

It is a pleasure to acknowledge M. Boninsegni, G. Gervais, R. Melko, and N. Prokof'ev for many fruitful and interesting discussions on various aspects of this study. This work was made possible through support from CIFAR (I.A.), NSERC (A.D.M. and I.A.) and the NRAC of Compute Canada with computational resources being provided by WESTGRID and SHARCNET.

¹F. D. M. Haldane, *Phys. Rev. Lett.* **47**, 1840 (1981).

²M. Greiner, I. Bloch, O. Mandel, T. W. Hänsch, and T. Esslinger, *Phys. Rev. Lett.* **87**, 160405 (2001).

³M. Boninsegni, A. B. Kuklov, L. Pollet, N. V. Prokof'ev, B. V. Svistunov, and M. Troyer, *Phys. Rev. Lett.* **99**, 035301 (2007).

⁴M. Savard, C. Tremblay-Darveau, and G. Gervais, *Phys. Rev. Lett.* **103**, 104502 (2009).

⁵G. Gervais (private communication).

⁶N. M. Urban and M. W. Cole, *Int. J. Mod. Phys. B* **20**, 5264 (2006).

⁷G. E. Astrakharchik and S. Giorgini, *Phys. Rev. A* **68**, 031602(R) (2003).

⁸M. Boninsegni, N. Prokof'ev, and B. Svistunov, *Phys. Rev. Lett.* **96**, 070601 (2006); M. Boninsegni, N. V. Prokof'ev, and B. Svistunov, *Phys. Rev. E* **74**, 036701 (2006).

⁹D. M. Ceperley, *Rev. Mod. Phys.* **67**, 279 (1995).

¹⁰ T dependent corrections coming from the restriction of the sum in Eq. (3) to $N \geq 0$ are exponentially small in N_0^2 , much smaller than those of $O(1/N_0)$ calculated here.

¹¹E. L. Pollock and D. M. Ceperley, *Phys. Rev. B* **36**, 8343 (1987).

¹²A. Del Maestro and I. Affleck (unpublished).

¹³A. Imambekov and L. I. Glazman, *Science* **323**, 228 (2009).

¹⁴R. G. Pereira *et al.*, *J. Stat. Mech.: Theory Exp.* (2007) P08022.

¹⁵J. Sirker *et al.*, *J. Stat. Mech.: Theory Exp.* (2008) P02015.

¹⁶T. Kinoshita, T. Wenger, and D. S. Weiss, *Nature (London)* **440**, 900 (2006).

¹⁷E. H. Lieb and W. Liniger, *Phys. Rev.* **130**, 1605 (1963).

¹⁸E. H. Lieb, *Phys. Rev.* **130**, 1616 (1963).